EVALUATION OF A TWO DIMENSIONAL CENTRIFUGAL PUMP IMPELLER

by

John H. Beveridge[1] and Dino A. Morelli[2]

Summary

The two-dimensional radial flow pump impeller has significant advantages for the study of the transfer and diffusion of energy. It is well adapted to experimental investigation and permits accurate and economical design modifications. The present study was undertaken to evaluate the essential limitations of a special series of two-dimensional impellers by photographic and hydrodynamic techniques which are described in the present paper and elsewhere. The head-capacity characteristics, losses and efficiency, are discussed in the light of visual evidence available from high speed motion pictures of the relative and absolute flow. The dominant influence of the inlet angle on the impeller performance is demonstrated.

Introduction

Under the continuing sponsorship of the Office of Naval Research, further studies have been made at the Hydraulic Machinery Laboratory of the California Institute of Technology on the flow in rotating channels. The previous work (1),* (2), done at the Laboratory, utilized high efficiency three-dimensional centrifugal pump impellers representing good modern practice. Their over-all performance in complete pumps had already been measured accurately for other purposes.

The knowledge gained in these studies made it desirable to develop a series of impellers which would permit detailed observation of the inlet edges of the vanes. From the standpoints of the least photographic distortion, maximum accessibility, and manufacturing ease, a radial impeller with parallel shrouds and general cylindrical vanes is indicated. The question arises that such impeller may be so inefficient that deductions made from the experimental results would be meaningless. Very careful consideration was given to this question in the development of the radial impeller used in the present work. The quality of the data and the character of the flow as depicted in high speed moving pictures have justified the unconventional design adopted.

---

[1] Research Engineer, Hydraulic Machinery Laboratory, California Institute of Technology.

[2] Senior Research Engineer, Hydraulic Machinery Laboratory, Assistant Professor, Mechanical Engineering, California Institute of Technology.

* Numbers in parentheses refer to bibliography at end of the paper.

It is not suggested that such an impeller is for use in a complete pump, but that it is of great value in a research program whose object is to isolate the individual effects of many variables.

The Test Impellers

The general dimensions adopted for the series of impellers are given in Fig. 1. The top shroud is made of lucite polished to a high transparency while the suction shroud is made from aluminum plate black anodized for better photographic background. Both shrouds are grooved to accurate templates to receive the six vanes of constant thickness which are made from 3/32" 2-S aluminum sheet. For greater utility each set of shrouds is milled to receive two sets of six vanes and the flutes not occupied by vanes are filled with wax before assembly. The complete impeller is held together by through-bolts at each vane tip. Figure 2(a) shows an impeller disassembled and Fig. 2(b) the assembled unit.

Shroud Shape

The unconventional shroud contour shown in Fig. 1 was adopted after an investigation of the potential flow in a three-dimensional axially symmetric turn. The short radius turn of the suction shroud permits the two-dimensional character of the impeller to be maintained well in towards the center, while the reverse curvature of the back shroud endows the flow pattern with near-symmetry at the inlet edges of the vanes.

Vane Shape

The outlet vane angle, β_2, was 23.5° for all the impellers of the series. The inlet angle was varied for each impeller and the vane shape is such that the tangential component of the absolute velocity at the design flow rate increases linearly with radius when calculated by assuming an infinite number of vanes. For the three units reported here the inlet vane angles, β_1, are 20°, 17.5°, and 15.0°, illustrated in Fig. 3. Each impeller will be denoted by the value of β_1.

Equipment and Technique

The general laboratory facilities and testing techniques have been described elsewhere (1), (2). The use of total head tubes rotating with the impeller and directed into the relative flow is a new technique of special interest. Air-liquid differential manometers are mounted on the impeller shaft truly parallel to the axis

of rotation. The centerlines of all tubes must be at the same distance from the axis. The lower end of one glass tube is connected to a total head tube directed into the approach flow at the axis of rotation. This tube forms the common leg of all the manometers through a manifold connecting the tops of all the tubes. The lower ends of all other tubes are connected to total head tubes mounted on the impeller at the outlet periphery and facing into the relative flow. Connecting tubes must be filled with the working fluid. The displacement of the liquid levels in the manometer is a direct measurement of the loss suffered by the fluid impinging on the outlet total-head tube in its passage through the impeller. Fig. 4(a) and 4 (b) show the arrangement used in the present tests to determine the distribution of losses in impeller passages.

Character of the Flow

By menas of high speed moving pictures and silk thread streamers the general quality of the flow through the impellers was examined. In the range of high efficiency the flow was very well behaved from inlet to outlet. Cross currents in the axial direction and variations with time were noticeably absent. This is in special contrast with previous studies (1). At very high flow rates distinct separation was noted on the pressure face of the vanes at the inlet edges.

At low flow rates the flow becomes much more complex. General turbulence becomes evident throughout the passages and asymmetric patterns develop in alternate passages. The development of asymmetry has been noted by Fisher and Thoma (4). Pulsations in the discharge also become pronounced in this zone of operation.

Head-Capacity Characteristics

The unit head, measured by a total head tube close to the vane tips , versus unit capacity, is shown in Fig. 5(a), 5(b), and Fig. 5(c).for the three impellers of the series. These diagrams show the kind of variation which occurs across the outlet width and the degree of symmetry which has been achieved by the shroud profiles used. Figure 6 is an average plot made from the data of Figs. 5(a), (b), (c).

The influence of the inlet angle on the characteristic is especially well-defined in the high capacity zone. The zero head point moves to the left as the inlet angle decreases and the bend in the curves which indicates separation on the pressure side of the vane behaves similarly. The high efficiency range of these impellers is shown in Fig. 7, which should be studied in close conjunction with Fig. 6.

The influence of inlet angle is less well defined in the low capacity range. Since the series was designed to have best efficiency at values of unit capacity less than 0.11, one would perhaps expect to find evidence of separation at the suction side of the vane at lower values of unit capacity. From all the curves of Fig. 6 it will be seen that the change of inlet angle produces very little change in the characteristic at low capacities. Figure 7 illustrates this still more strongly; while the right hand branch of the efficiency curves moves left with decreasing inlet angle as would be expected, the left-hand branch does not. This leads to the conclusion that the behavior of the impeller to the left of a unit capacity of 0.1 does not depend entirely on the inlet angle.

In an earlier publication (1), it was noted that measurements of head by a total head tube located some distance from the vane tips gave results significantly lower than those obtained by a tube close to the tips. Part of this deficiency was later ascribed (2) to a crossflow at the outlet, which caused errors in the total head readings. Such crossflows were not found in the present series of impellers; Fig. 8 shows the effect of location of the total head tube on the outlet head measured and is typical for all three impellers. The readings for the total head tube at 3/8" distance from the vane tips fall below the data obtained at 1/16" distance in two regions. The region at the right is where separation exists on the pressure side of the vane. The point of separation of the two curves for the region at the left did not show significant dependence on the inlet vane angle. It is practically at the same location for all three impellers.

Figure 9 shows the average close-in head capacity curve for the 20° impeller. On the same diagram the head calculated from the measured horsepower is drawn and marked as "indicated total head." For this impeller the best efficiency point is at $\frac{C_{m2}}{\mu_2} = 0.1$.

Between $\frac{C_{m2}}{\mu_2} = 0.1$ and $\frac{C_{m2}}{\mu_2} = 0.15$ the vane is operating under good entrance conditions and the hydraulic losses are usually assumed approximately proportional to the square of the velocity. To the contrary, Fig. 9 shows that the measured hydraulic losses are almost constant in the range of satisfactory inlet conditions.

Spannhake has noted (3) that the statement of hydraulic losses through an impeller as a function of the square of velocity is untenable. The authors submit that an induced vorticity loss due to the motion of the boundaries is of importance at the low flow rates. This loss determines the trend of the head-capacity curve and the possible efficiency attainable at very low values of unit capacity. Since the induced vorticity loss depends on kinematic viscosity, it is

expected that the point at which this effect becomes important depends on Reynolds number.

Direct Measurement of Losses

For a clearer understanding of the origin and distribution of losses in the flow through the impeller, recourse was taken to direct measurements. The technique has been described briefly earlier in this paper.

In the range of high efficiency, the distribution of losses for the 20° impeller is shown in the loss contour plot, Fig. 10(d). The numbers on the contours are percentages of the indicated head at the flow rate at which the measurements were made and it is seen that the losses are high on the suction side of the vane where the velocities are high, and very low on the pressure side.

At high flow rates, beyond the point at which the flow separates on the pressure face at the inlet, the loss distribution at the periphery of the impeller is shown in Fig. 10(f). High losses appear at the pressure side as well as on the suction side of the vane, and the band of high loss flow on the suction side has been compressed into a narrow zone by the separated flow at the other side of the passages. It is interesting to note the tendency for high-loss fluid on the pressure face to move to the bottom of the passage.

Figures 10(a), 10(b) and 10(c) are of very great interest because in none of these is there any evidence of complete separation on the suction side of the vane. The data from which these figures were compiled show that complete separation occurs around $\frac{C_{m2}}{\mu_2} = 0.05$ for this impeller and some evidence has been found of local separation on the suction side of the vane near the inlet at a capacity of 0.07.

Furthermore, the percentage loss does not increase significantly as the flow rate is decreased from Figs. 10(c) to 10(a). However, since the indicated head increases with decreasing flow rate the absolute value of the losses increases from Fig. 10(c) to 10(a). This increase cannot be explained by losses which vary as the square of velocity, but can be explained reasonably in terms of induced vorticity loss due to the motion of the boundaries. The general increase of losses in the center of the passage substantiates still further the latter explanation.

Efficiencies calculated from the losses are in good agreement with the measured efficiencies in the zone of high efficiency. At lower flow rates the calculated values are higher than the measured values. This leads to the belief that at the outer perimeter of the

impeller large mixing losses occur at low flow rates. This has already been inplied in a previous paragraph where it was noted that at low flow rates, the average measured head is less when the total head tube is located some distance away from the vane tips (Fig. 8). Detailed investigation of this point is the subject of current experimental study.

Figures 11(a) and 11(b) are loss contours taken at 3.9" radius and at the periphery (5.15" radius) in the 15° impeller at a high flow rate. They show how the high loss fluid flowing along the pressure face emerges at the outlet at the bottom shroud. At this capacity, the flow separates at the inlet on the pressure face of the vane, and it appears that the separation occurs somewhat earlier near the lower shroud. This asymmetry induces a crossflow in the passage which results in the configuration of losses at the outlet shown in Fig. 11(b).

Jump in Head-Capacity Characteristic

High efficiency three-dimensional impellers, reported in references (1) and (2), show a discontinuity in the head-capacity characteristic at a flow rate below the design condition. Tests with increasing and decreasing flow rates do not give identical results in the neighborhood of this discontinuity, but plot as a loop in the curve.

Distinct discontinuities have not been found in the impellers reported in this paper, and the loop in the head-capacity curve, if it exists, is of the order of the experimental scatter of the data. The presence or absence of the loop cannot be definitely established by these data. The shut-off head in the impellers of this series is lower by a significant amount than that of the equivalent impeller of the three-dimensional series reported in reference (2).

These radical differences in behavior between the two-dimensional and three-dimensional impellers of substantially the same specific speed can be attributed mostly to the very great difference in the design of the inlet. The discontinuity in the head-capacity curve in three-dimensional impellers can be readily associated with local separation at one end of the skew leading edge which can induce backflow into the approach pipe. This backflow can be pictured as a circulating flow in the axial plane. The flow ratio at which such a separation occurs when decreasing the flow, is not necessarily identical with the flow rate at which it will disappear when the flow is increased.

At shut-off the forced vortex head is determined by the inner and outer radii of the forced vortex. In the two-dimensional impellers no rotation in the eye has been observed at shut-off. The same cannot be said for three-dimensional impellers. All were tested

without volute casings. The three-dimensional impellers have vanes which extend well into the eye and must necessarily produce greater shut-off head than the two-dimensional units.

Conclusion

The data and their interpretation show that the two-dimensional impeller is not essentially inefficient. In spite of the narrow inlet which is a consequence of the parallel shrouds, the efficiency is high. A wider inlet will reduce the hydraulic losses and increase the efficiency a little. It will also increase the length of the vanes which are already long by current standards. A wider inlet will have the important effect of increasing the width of the high efficiency range and broaden the base of the unit characteristic.

Acknowledgements

For the many helpful suggestions of the general laboratory staff under the direction of Dr. Robert T. Knapp, and particularly for the assistance and cooperation of those staff members directly connected with this project, grateful acknowledgement is given.

BIBLIOGRAPHY

(1) Osborne, W.C. and Morelli, D.A., "Head and Flow Observations on a High Efficiency Centrifugal Pump Impeller", Trans. A.S.M.E., Vol. 72, 1950, pp. 999-1006.

(2) _____, "Measured Performance of Pump Impellers", Preprint no. 50-A-90, to be presented at Annual Meeting ASME, Nov. 26-Dec. 1.

(3) Spannhake, Wilhelm, "Centrifugal Pumps, Turbines and Propellers", The Technology Press, M.I.T., Cambridge 1934, p. 251.

(4) Fisher, K. and Thoma, D., "Investigation of the Flow Conditions in a Centrifugal Pump", Trans. A.S.M.E., Vol. 54, 1932, p. 141.

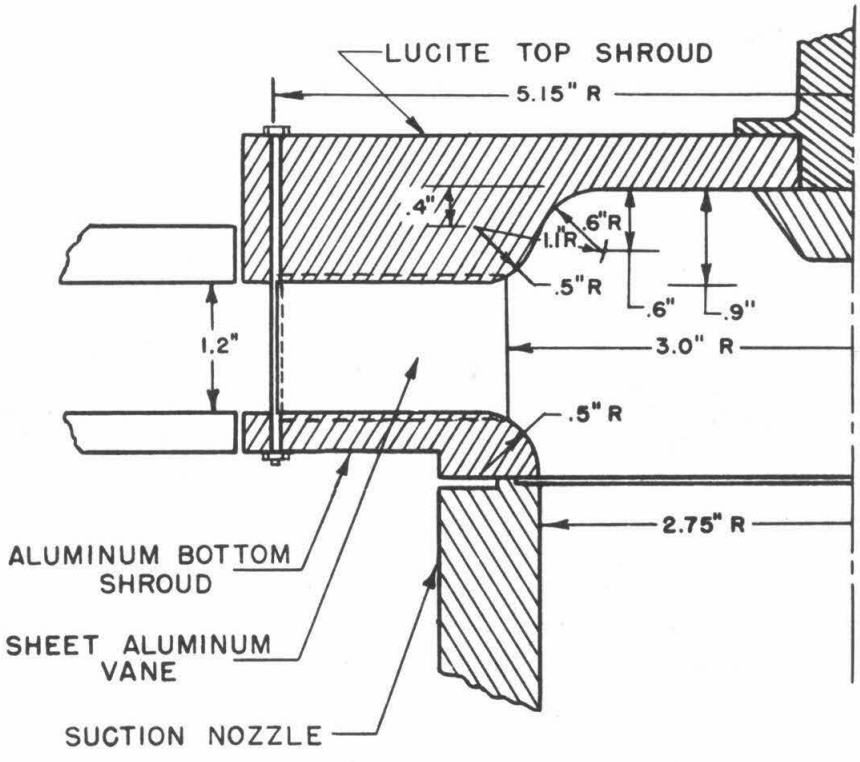

Fig. 1 Axial cross-section of a typical impeller

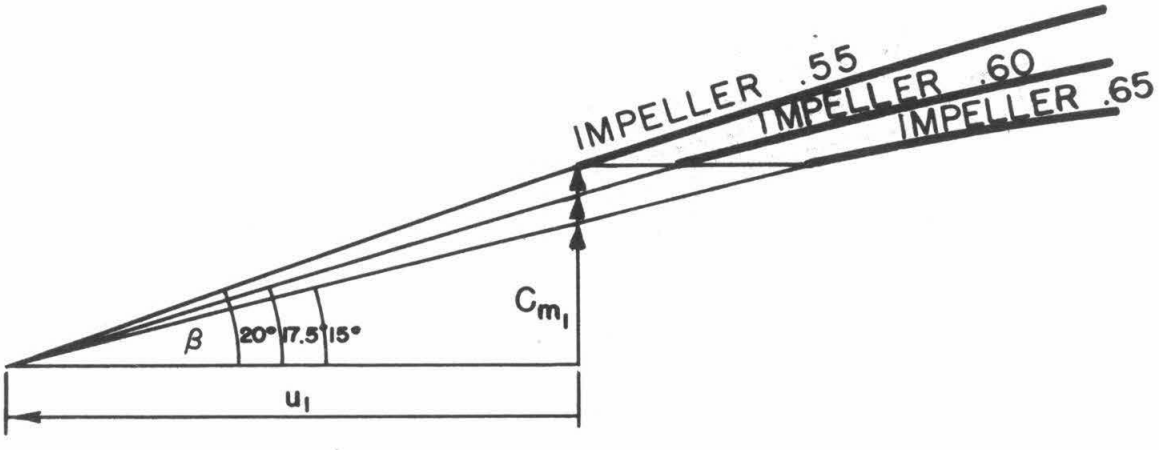

Fig. 3 Inlet angle β, for three impellers.
Design unit capacities 0.105, 0.091, 0.077

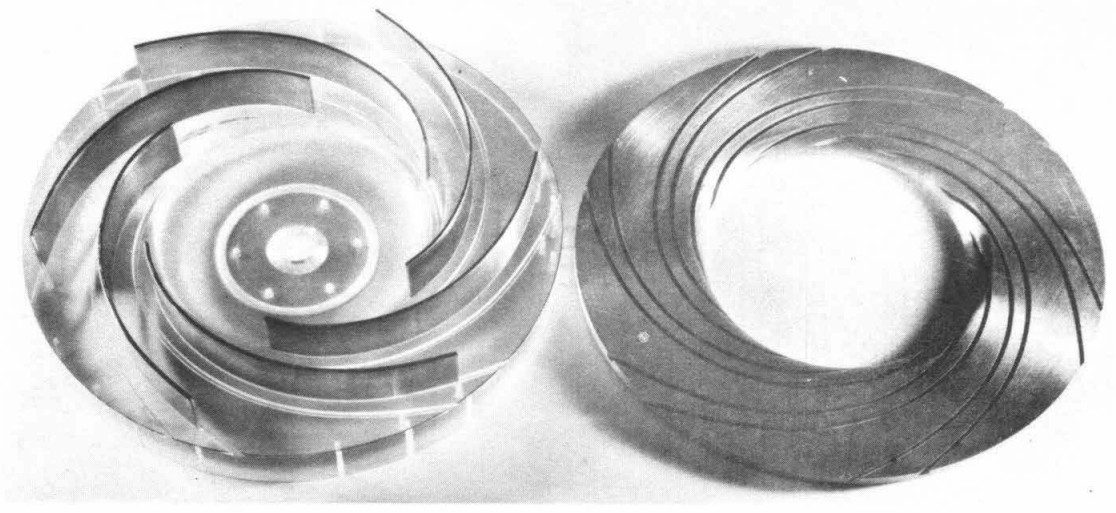

Fig. 2 (a) Disassembled view of 15° impeller

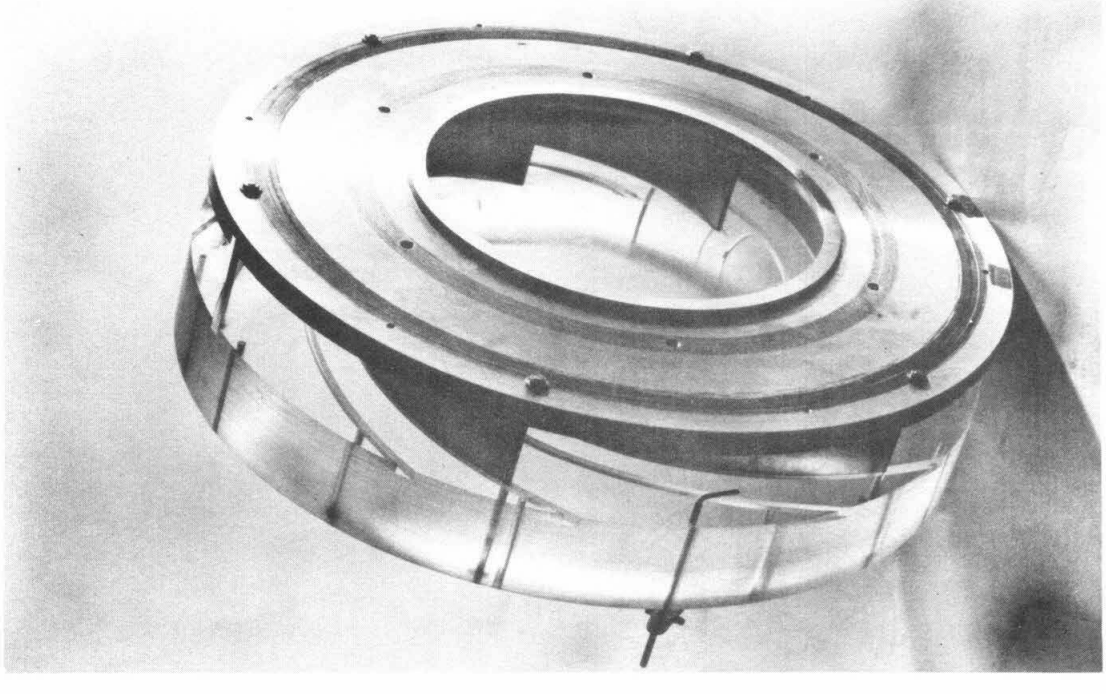

Fig. 2 (b) Assembled view of 15° impeller with one relative total-head tube in position

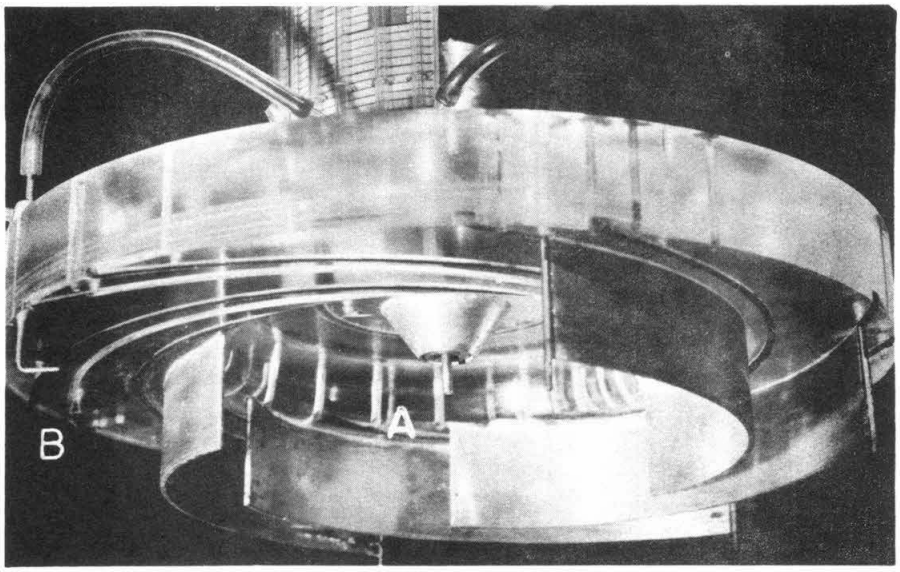

Fig. 4 (a) View of relative total head tubes. The relative total suction head tube in the eye is marked "A". The relative total head tube in the passage is indicated by "B". The lower shroud and two vanes have been removed.

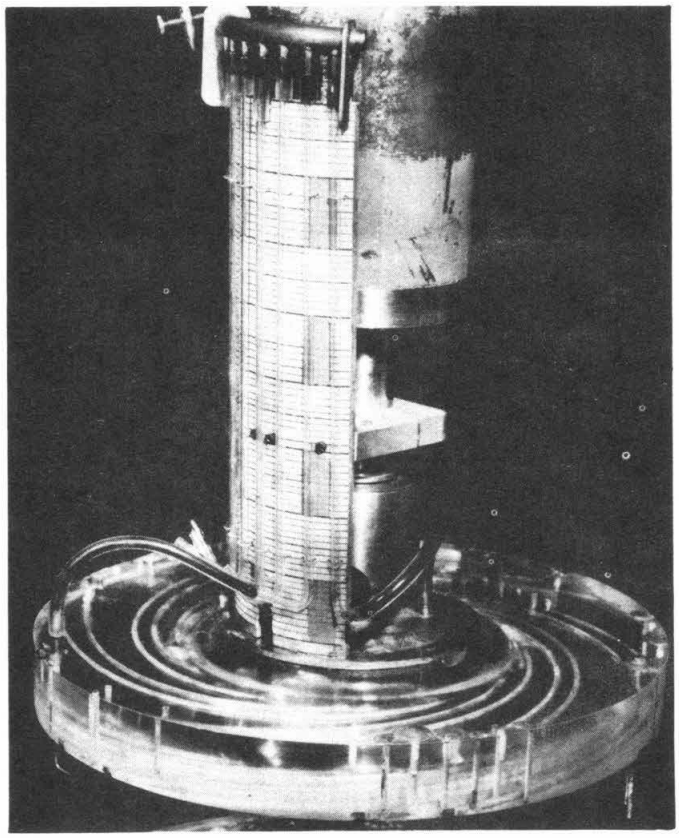

Fig. 4 (b) The manometer mounted to the dynamometer shaft rotates at impeller speed. The relative total head tube in the eye is differentially connected to the relative total head tube in the discharge.

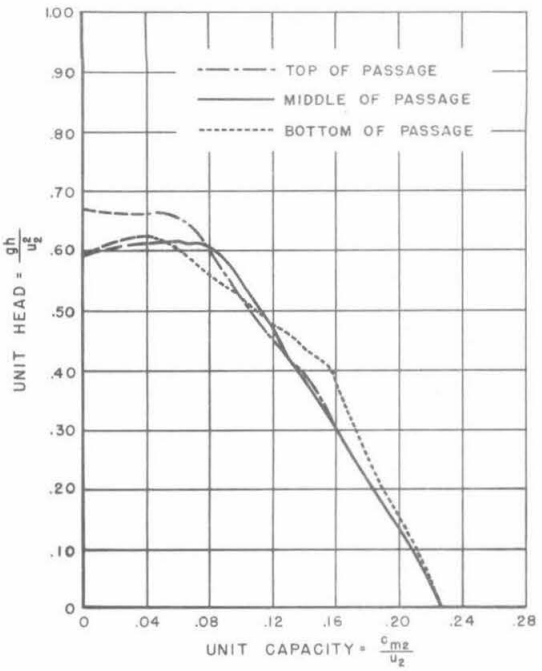

Fig. 5 (a) Unit head vs. unit capacity at three locations across the outlet width.
20° impeller

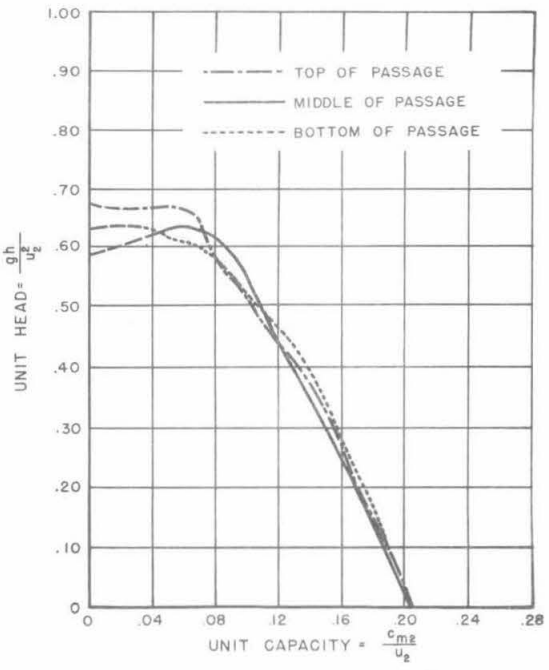

Fig. 5 (b) 17.5° impeller

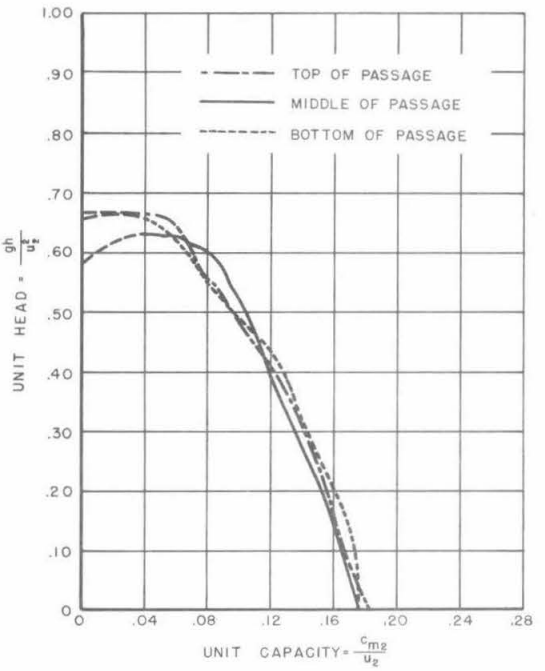

Fig. 5 (c) 15° impeller

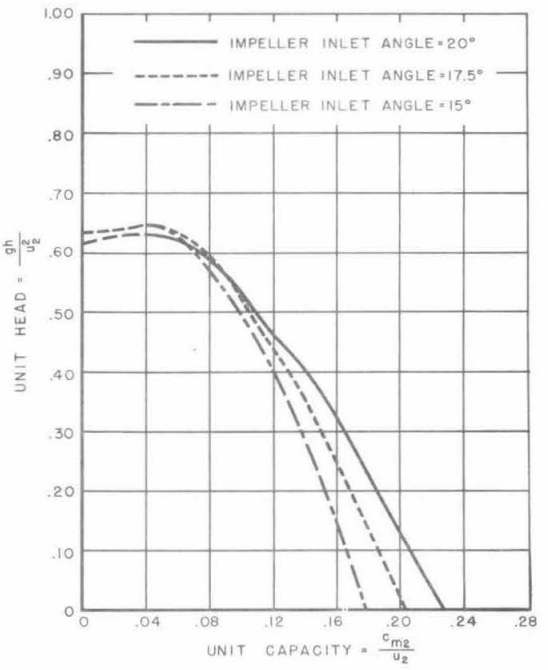

Fig. 6 Average unit head vs. unit capacity for three impellers. Head measured 1/16" from vane tip.

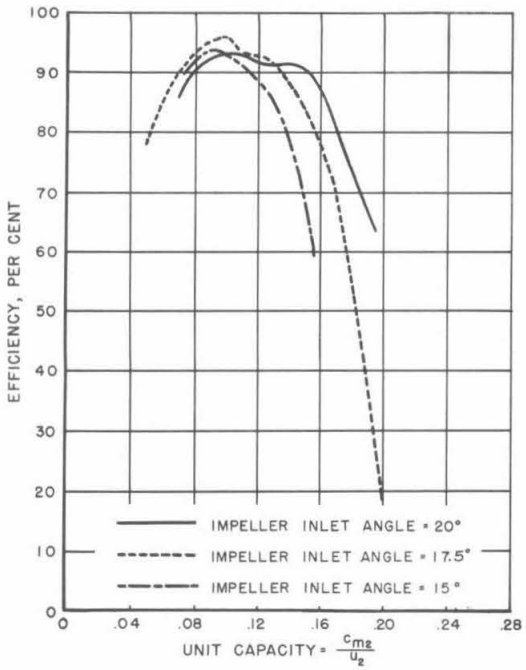

Fig. 7 Efficiency vs. unit capacity for three impellers based on head measure at 1/16" from vane tip.

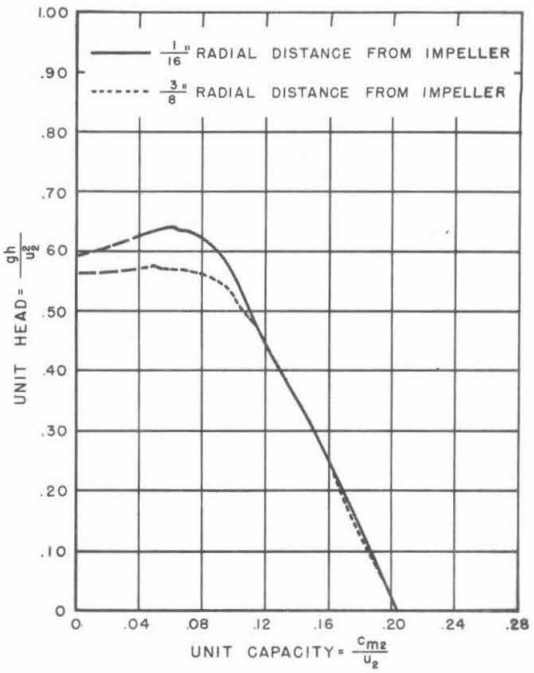

Fig. 8 Effect of radial distance on the measured head.

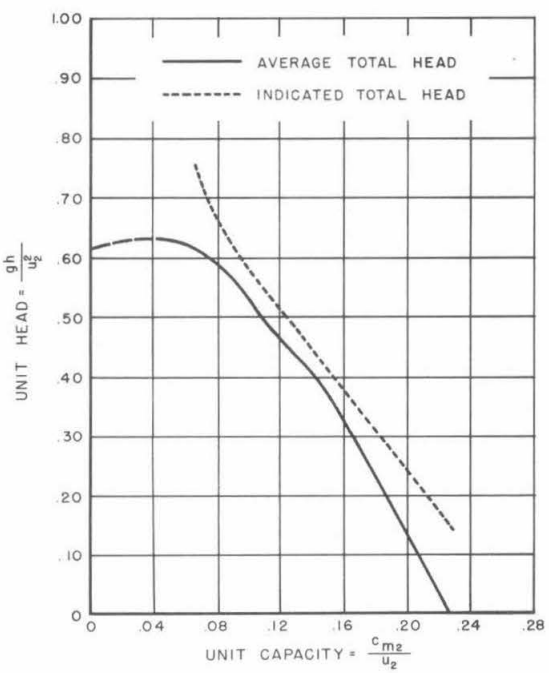

Fig. 9 Losses for the 20° impeller shown as a deficiency in unit head. Indicated total head is calculated from the measured horsepower.

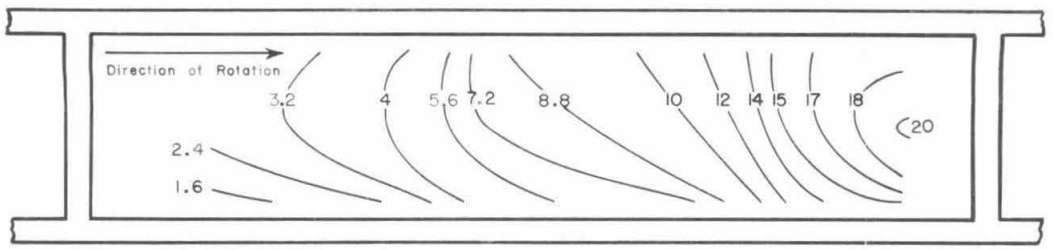

Fig. 10 (a) Percentage loss contours for the 20° impeller at various flow rates plotted on the developed perimeter

$$\frac{C_{m2}}{\mu_2} = 0.061$$

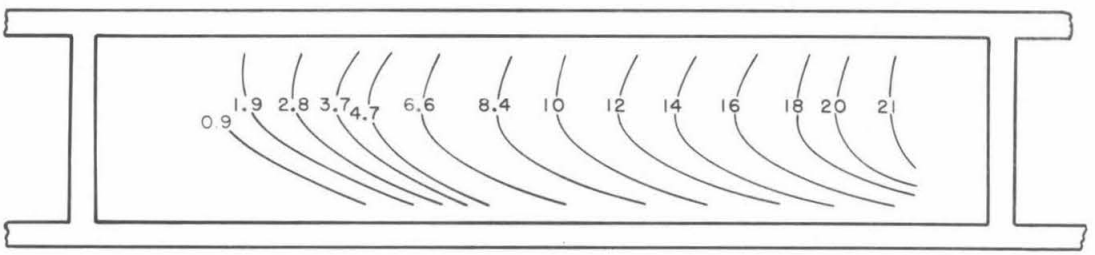

Fig. 10 (b) $\frac{C_{m2}}{\mu_2} = 0.078$

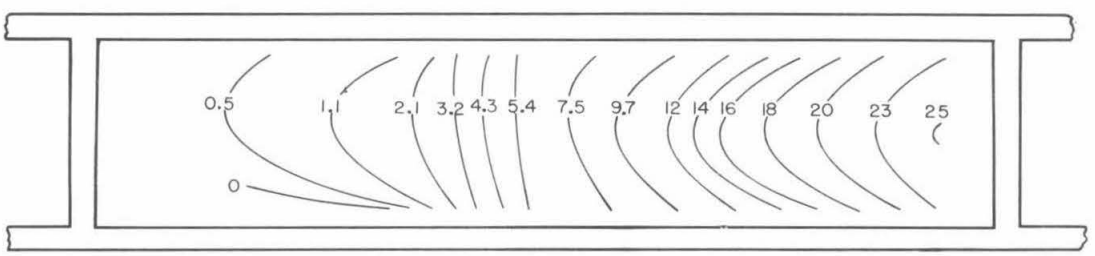

Fig. 10 (c) $\frac{C_{m2}}{\mu_2} = 0.098$

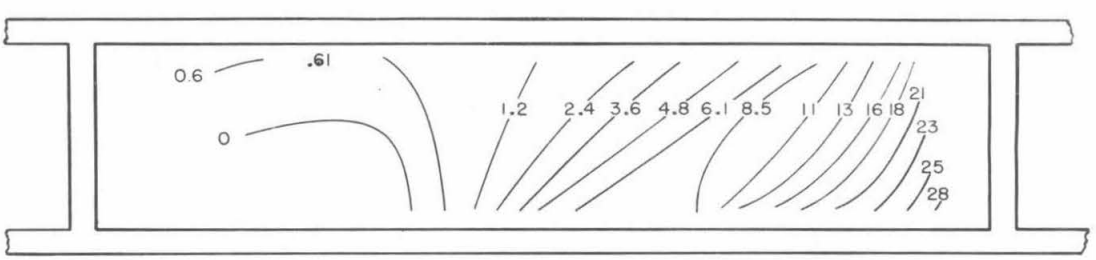

Fig. 10 (d) $\frac{C_{m2}}{\mu_2} = 0.118$

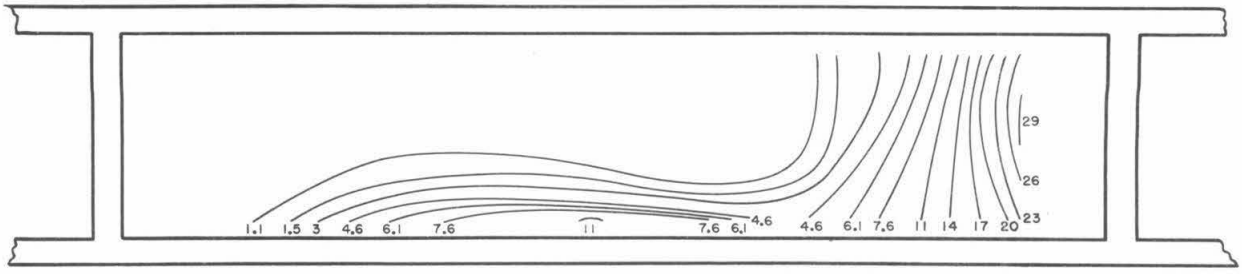

Fig. 10 (e) $\frac{C_{m2}}{\mu_2} = 0.150$

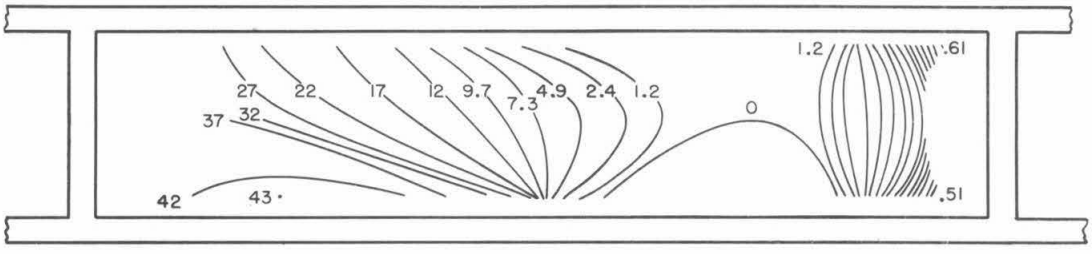

Fig. 10 (f) $\frac{C_{m2}}{\mu_2} = 0.195$

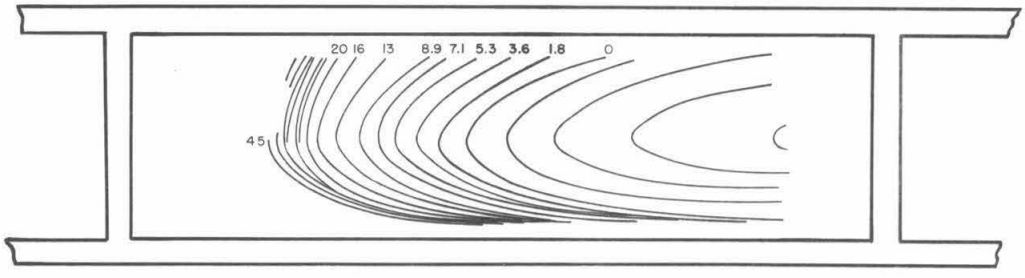

Fig. 11 (a) Percentage loss contours for the 15° impeller at two radii 3.9" radius

$\frac{C_{m2}}{\mu_2} = 0.150$

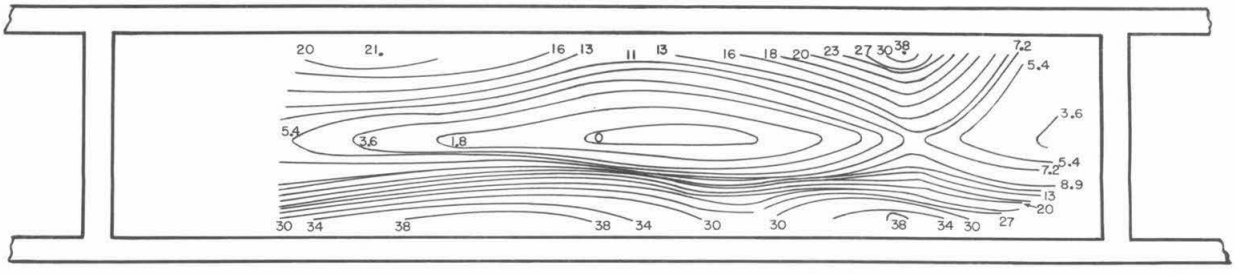

Fig. 11 (b) 5.15" radius (periphery)

$\frac{C_{m2}}{\mu_2} = 0.150$